TISSUE ENGINEERING: Part A
Volume 20, Numbers 21 and 22, 2014

DOI: 10.1089/ten.tea.2013.0614

Enhanced Chondrogenic Differentiation of Dental Pulp Stem Cells Using Nanopatterned PEG-GelMA-HA Hydrogels

Cameron L. Nemeth,[1,*] Kajohnkiart Janebodin, DDS, PhD,[2–4,*] Alex E. Yuan,[1] James E. Dennis, PhD,[5] Morayma Reyes, MD, PhD,[2,3,6] and Deok-Ho Kim, PhD[1,3]

We have examined the effects of surface nanotopography and hyaluronic acid (HA) on *in vitro* chondrogenesis of dental pulp stem cells (DPSCs). Ultraviolet-assisted capillary force lithography was employed to fabricate well-defined nanostructured scaffolds of composite PEG-GelMA-HA hydrogels that consist of poly(ethylene glycol) dimethacrylate (PEGDMA), methacrylated gelatin (GelMA), and HA. Using this microengineered platform, we first demonstrated that DPSCs formed three-dimensional spheroids, which provide an appropriate environment for *in vitro* chondrogenic differentiation. We also found that DPSCs cultured on nanopatterned PEG-GelMA-HA scaffolds showed a significant upregulation of the chondrogenic gene markers (*Sox9, Alkaline phosphatase, Aggrecan, Procollagen type II,* and *Procollagen type X*), while downregulating the pluripotent stem cell gene, Nanog, and epithelial–mesenchymal genes (*Twist, Snail, Slug*) compared with tissue culture polystyrene-cultured DPSCs. Immunocytochemistry showed more extensive deposition of collagen type II in DPSCs cultured on the nanopatterned PEG-GelMA-HA scaffolds. These findings suggest that nanotopography and HA provide important cues for promoting chondrogenic differentiation of DPSCs.

Introduction

A current challenge in tissue engineering is to create a microengineered extracellular matrix (ECM) that can direct cell adhesion, proliferation, and differentiation similar to *in vivo* conditions.[1] Nanofabrication of the topographical environment has shown promise in directing cell orientation, geometry, and adhesion similar to that observed *in vivo*.[2–4] Numerous studies have demonstrated the use of biomaterials to create tissue scaffolds with nanoscale topographical cues to elicit behavior in cells that more closely resembles that observed in native tissue.[5–7]

Many contemporary techniques for fabricating biomaterial scaffolds with nanoscale features include electrospinning, nanoimprinting, dip-pen nanolithography, and capillary force lithography (CFL).[8–10] Of these methods, only CFL is capable of generating well-defined nano-features over large areas without the need of expensive or sophisticated equipment.[11] In CFL, capillary action is used to draw a solution of polymerizable monomers into a mold. The monomers are then polymerized, typically with heat, the removal of a solvent, or ultraviolet (UV) light.[12] The simple and inexpensive generation of scaffolds with precise nano-features allows facile detection of sensitive cell responses to the nanotopographical environment.

In addition to providing topographical signals, native ECM provides chemical cues to cells through the presentation of proteins, sugars, and glycosaminoglycans (GAGs) embedded in the ECM architecture.[13] Hyaluronic acid (HA) is a naturally occurring GAG and is an integral part of the ECM in cartilage tissue and is the most prevalent ECM molecule in the synovial fluid.[14] HA provides cells with numerous biochemical cues, mediated by receptors such as CD44 and RHAMM, to regulate the behavioral aspects of cells such as morphology, proliferation, and migration.[15,16] HA has also been found to provide chemical cues to promote stem cell

Departments of [1]Bioengineering and [2]Oral Health Sciences, University of Washington, Seattle, Washington.
[3]Center for Cardiovascular Biology, Institute for Stem Cell and Regenerative Medicine, University of Washington, Seattle, Washington.
[4]Department of Anatomy, Faculty of Dentistry, Mahidol University, Bangkok, Thailand.
[5]Benaroya Research Institute at Virginia Mason, Seattle, Washington.
[6]Department of Pathology, University of Washington, Seattle, Washington.
*These authors contributed equally.

differentiation toward the chondrogenic lineage and is used in currently available cartilage repair therapies.[17,18]

Mesenchymal stem cells (MSCs) can differentiate into chondrocytes and deposit cartilage matrix in either cell monolayer (two-dimensional) or cell aggregate (three-dimensional [3D]) cultures.[19,20] Dental pulp stem cells (DPSCs) are well-characterized neural crest-derived MSCs that are isolated from both human and murine tooth pulp.[21,22] DPSCs are an attractive postnatal stem cell source as they are easily accessible, can be easily expanded *ex vivo*, and exhibit multipotency and regenerative capacity, whereas extraction of MSCs requires an invasive procedure and MSCs exhibit less expansion capacity than do DPSCs.[23–25] Murine DPSCs are derived from neural crest origin and express the epithelial–mesenchymal transition (EMT) genes, *Twist*, *Snail*, and *Slug*.[21] These EMT genes have been shown to be important for inhibition of chondrogenesis both *in vitro* and *in vivo*, whereas downregulation of EMT genes enhances chondrogenic differentiation.[26–28] *In vitro* differentiation using induction media supplemented with growth factors, such as bone morphogenetic protein (BMP) or transforming growth factor (TGF)-β, can induce MSCs to differentiate into the chondrogenic lineage as shown by increased levels of chondrogenic genes and proteins.[20,29] DPSCs can differentiate into chondrocytes under appropriate stem cell niches, which may require downregulation of the expression levels of EMT genes. The easy accessibility, tremendous *ex vivo* expansion capacity, and malleability for efficacious differentiation make DPSCs a promising MSC source for cartilage tissue engineering.

Efforts to regulate the chondrogenic differentiation of stem cells have shown that stem cell behavior is largely dependent on mechanical and chemical cues from the extracellular environment.[30,31] The importance of composite hydrogels has been established in replicating the natural ECM and providing the signals necessary for cartilage differentiation.[32] The structure of cartilage is composed of multiple layers with different cellular organizations. In the superficial layer, chondrocytes are well aligned. Previous groups have demonstrated the use of anisotropic scaffolds to mimic the superficial layer for articular cartilage regeneration.[33,34] It has also been demonstrated that nanotopography can be responsible for the formation of 3D growth of cell structures.[35] In the field of cartilage tissue engineering, spheroid formation provides a 3D architecture that enhances chondrogenic differentiation capacity.[36,37] Previous studies have demonstrated that HA and 3D spheroid culture systems using photolithography techniques can promote MSCs to form spheroids.[23,38] Motivated by the urgent need for more efficient cartilage tissue engineering platforms and by the potential of stem cell-based therapies, we sought to assess the combined effects of matrix nanotopography and HA-mediated signaling on the chondrogenic differentiation of DPSCs. We chose to use CFL for nanofabrication due to its low cost, ease of use, and the ability to be fabricated into a diverse array of structures. To facilitate UV curing, we conjugated thiol-modified HA to poly(ethylene glycol) dimethacrylate (PEGDMA). We then cultured DPSCs on scaffolds in the BMP-2-supplemented medium and determined their capacity to differentiate by examining the expression of chondrogenic genes and proteins. In this study, we first report that nanopatterned PEG-GelMA-HA scaffolds fabricated by CFL enhance spheroid formation and chondrogenic differentiation of DPSCs.

Materials and Methods

Synthesis of PEG-GelMA-HA precursor solution

Synthesis of the PEG-GelMA-HA precursor solution was completed in two steps: (i) preparation of gelatin methacrylate and (ii) conjugation of HA and methacrylated gelatin (GelMA) to PEGDMA (Polysciences). Synthesis of GelMA was conducted as previously described.[39] Briefly, gelatin (Sigma-Aldrich) was added at 10% (w/v) to Dulbecco's phosphate-buffered saline (DPBS; Sigma-Aldrich) at 60°C in stirring condition until a clear mixture was observed. Methacrylic anhydride (Sigma-Aldrich) was added at 50°C to form a 20% (w/v) solution. DPBS was added to dilute and stop the reaction after 2 h. The solution was subsequently dialyzed through a porous membrane bag (12–14 kDa molecular weight cutoff; Spectrum Lab, Inc.) to remove residual salts and methacrylic acid in deionized water. The resultant product was filtered through a 22-μm membrane (Millipore) and lyophilized for 4 days to produce white porous foam. To form a PEG-GelMA-HA precursor solution, PEGDMA (M_w 1.0×10^4 Da) was suspended in the DPBS solution, then mixed with lyophilized GelMA, and suspended Glycosan HyStem, a thiol-modified HA product (M_w 2.4×10^5 Da, generously provided by BioTime, Inc.). Twenty percent of PEGDMA (w/v) was prepared with 10% GelMA (w/v) and 0.5% HA (w/v). The solution was mixed thoroughly by vortexing. The photoinitiator 2-hydroxy-2-methylpropiophenone (Sigma-Aldrich) was subsequently added at 1% (v/v). The precursor solution was covered in aluminum foil until further use.

Fabrication of nanopatterned PEG-GelMA-HA hydrogels

Glass coverslips (BioScience Tools) were cleaned in a piranha solution consisting of a 3:1 ratio of 100% sulfuric acid (Sigma-Aldrich) and 30% aqueous hydrogen peroxide (Sigma-Aldrich) for 30 min to remove organic material and provide additional hydroxyl groups before silane treatment. Then, coverslips were thoroughly cleaned using deionized water and dried under an air stream before being submerged in 2 mM 3-(trimethoxysilyl) propyl methacrylate (Sigma-Aldrich) in anhydrous toluene (Sigma-Aldrich) for 60 min. The glass coverslips were rinsed in toluene again and dried under an air stream. The cleaned and silane-treated coverslips were stored under vacuum inside a desiccator until used. UV curable nanopatterned polyurethane acrylate (PUA) (Minuta Tech) molds were prepared for fabrication. Characterization and synthesis were previously described.[5] The PUA mold consisted of a pattern of ridge × groove × height dimensions of $800\times800\times500$ nm. Anisotropically nanopatterned PEG-GelMA-HA hydrogels were fabricated on the pretreated glass coverslips using UV-assisted CFL. A PUA mold was rinsed with 100% ethyl alcohol to remove organic contaminants and was carefully placed onto the surface. A small amount (~10 μL) of PEG-GelMA-HA precursor solution was pipetted onto a single glass coverslip. The solution was drawn into the nanogrooves of the pattern through capillary action and cured by exposure to UV light ($\lambda = 365$ nm) for 5 min. After curing, the PUA mold was peeled off leaving a nanopatterned PEG-GelMA-HA hydrogel scaffold.

Characterization of PEG-GelMA-HA hydrogels

The surface topography of PEG-GelMA-HA hydrogels was analyzed by a high-resolution scanning electron microscope (FEI Sirion SEM). Images were taken of hydrogels with and without patterning. To confirm the presence of HA on PEG-GelMA-HA hydrogels scaffolds, toluidine blue staining was conducted on both the PEG-GelMA and PEG-GelMA-HA scaffolds. Toluidine blue is a metachromatic chemical dye used to detect GAGs.[40] Briefly, 1% toluidine blue (w/v) was prepared in 70% ethanol and then diluted into 0.1% (w/v) in 1% NaCl. The PEG-GelMA-HA hydrogel scaffolds were stained in a toluidine blue solution for 15 min, washed three times with distilled water, and dried before image acquisition. The percentage area of positive toluidine blue staining was measured using ImageJ software analysis (NIH). X-ray photoelectron spectroscopy (XPS) spectra were taken on a Surface Science Instruments S-probe spectrometer. The X-ray spot size for acquisitions was $\sim$800 mm. The Service Physics Hawk Analysis Software was used to determine peak areas. The binding energy scales of the high-resolution spectra were calibrated by assigning the lowest energy C1s high-resolution peak a binding energy of 285.0 eV.

Morphological cell analysis

Cell orientation was determined on unpatterned and patterned scaffolds. The reference axis value of 0° indicates parallel alignment with the nanopattern, whereas 90° indicates perpendicular alignment with the nanopattern. The cell orientation angle was determined by the angle between the reference axis and the axis of the maximal cell cross-sectional length. The cellular elongation was determined as a ratio between cell length/cell width. Cell morphological measurements were conducted using ImageJ software analysis.

Cell culture

DPSC clones were previously isolated from 4- to 8-day-old neonatal mouse molar teeth under approved Institutional Animal Care and Use Committee (IACUC) guidelines and characterized.[21] Frozen cells were thawed and expanded (1500 cells/cm^2) in stem cell media containing 60% low-glucose Dulbecco's modified Eagle's medium (DMEM; Gibco, Invitrogen), 40% MCDB201 (Sigma-Aldrich), 2% fetal calf serum (FCS) (HyClone), insulin–transferrin–selenium (ITS) (Sigma-Aldrich), linoleic acid with bovine serum albumin (LA-BSA) (Sigma-Aldrich), 10^{-9} M dexamethasone (Sigma-Aldrich), 10^{-4} M L-ascorbic acid (Sigma-Aldrich), 100 units/mL penicillin with 100 mg/mL streptomycin (HyClone), 1×10^3 units/mL leukemia-inhibitory factor (LIF-ESGRO; Millipore), 10 ng/mL epidermal growth factor (EGF; Sigma-Aldrich), and 10 ng/mL platelet-derived growth factor (PDGF)-BB (R&D Systems) at 37°C under 5% O_2 and 5% CO_2.

DPSCs (20,000 cells/cm^2) were plated on tissue culture polystyrene (TCPS) and poly(ethylene glycol) (PEG)-based scaffolds, which were fabricated on 12-well plates in stem cell media. After 2 days, spheroids were collected and replated on TCPS surfaces under the same culture condition to observe cell survival and migration. The numbers of spheroids were counted after 2 and 6 days replating in culture. Spheroid-derived and replated cells were also collected for RNA. Details are summarized in Supplementary Figure S1 (Supplementary Data are available online at www.liebertpub.com/tea).

Quantification of cell viability through mitochondrial dehydrogenase activity

Cell viability of DPSCs seeded on different types of scaffolds ($n=3$) was determined through the mitochondrial dehydrogenase enzyme activity by using water soluble tetrazolium salt (WST-1) assay (Clontech). Briefly, 100 μL of premixed WST-1 cell proliferation solution was added to cells cultured in a glass-bottomed dish (Live Assay, Inc.) containing 1 mL of cell culture medium. After incubation at 37°C in 5% CO_2 for 4 h, 100 μL of the medium was transferred to a 96-well plate with a triplicate per scaffold condition. The absorbance at 450 nm was measured with a standard plate reader (VICTOR3V; PerkinElmer, Inc.). The total mitochondrial dehydrogenase activity increases proportionally to the number of viable cells, leading to an increase in absorbance values, which resulted from the enzymatic cleavage of the tetrazolium salt WST-1 to formazan.

In vitro *chondrogenic differentiation*

DPSCs (20,000 cells/cm^2) were plated on TCPS and PEG-based scaffolds, which were fabricated on 12-well plates and incubated overnight in stem cell media at 37°C under 5% O_2 and 5% CO_2. After 24 h, a spheroid formation was observed and the medium was switched to the BMP-2 medium for 10–21 days. The BMP-2 medium consisted of 60% low-glucose DMEM, 40% MCDB201, 10% FCS, ITS, LA-BSA, 10^{-7} M dexamethasone, 0.3 mM L-ascorbic acid, 100 units/mL penicillin with 100 mg/mL streptomycin, supplemented with 100 ng/mL BMP-2 (Shenandoah Biotech).[29] The BMP-2 medium was changed every 3 days. After differentiation, cells were collected for RNA and fixed for collagen type II antibody staining.

RNA extraction and quantitative reverse-transcriptase polymerase chain reaction

Total RNA was purified from DPSCs cultured in growth media and BMP-2 media with an RNeasy Mini kit (Qiagen), according to the manufacturer's protocol. Quantity and purity of RNA was determined by 260/280 nm absorbance. First-strand cDNA was synthesized from 1 μg of RNA using the High Capacity cDNA synthesis kit from Applied Biosystems as per the manufacturer's protocol using a randomized primer. Quantitative reverse-transcriptase polymerase chain reaction (QRT-PCR) primers are listed in Supplementary Table S1. cDNA (20 ng) was prepared using the SYBR green PCR master mix from Applied Biosystems. Reactions were processed by the ABI 7900HT PCR system with the following parameters: 50°C/2 min and 95°C/10 min, followed by 40 cycles of 95°C/15 s and 60°C/1 min. Results were analyzed using the SDS 2.2 software, and relative expression calculated using the comparative Ct method and normalized with *Gapdh* expression. Each sample was run in triplicate reactions for each gene.

Immunofluorescence

Cells were fixed with 4% formaldehyde in phosphate-buffered saline (PBS) for 10 min, washed with 1% BSA in 0.1% Triton X-100 in PBS, blocked with 10% normal goat

serum at room temperature (RT) for 1 h, and stained with either rat anti-mouse CD44 monoclonal Ab (1:100; eBioscience) or mouse anti-mouse collagen type II monoclonal Ab (1:500; Chondrex), incubated overnight at 4°C followed by three washes in PBS. Goat-derived anti-rat or mouse Alexa 594-conjugated secondary antibodies (1:800; Invitrogen) were incubated at RT for 1 h and washed three times. Cells were stained with 4′,6-diamine-2-phenylindol (DAPI) at 1:1000 to visualize the nuclei. All antibodies were diluted in 1% BSA in 0.1% Triton X-100 in PBS. The IgG isotypes from the species made for the primary antibody (0.1 μg/mL) (Vector Burlingame) were used as negative controls. Fluorescence micrographs were examined by a Zeiss Axiovert 200 fluorescence microscope. Images were taken with an onboard monochrome AxioCam camera. The background was reduced using brightness and contrast adjustments, and color balance was performed to enhance colors. Control images were treated the same as experimental images. All modifications were applied to the whole image using Adobe Photoshop CS2. The relative intensity collagen type II staining per cell was measured using ImageJ software analysis. The number of samples for the image analysis was three samples per scaffold group ($n = 3$). From each scaffold, five images were used for the analysis.

Statistical analysis

Quantitative data were analyzed using Student's *t*-test, one-way ANOVA, or Pearson's chi-squared test. *p*-Values <0.05 were considered statistically significant. All values are reported as mean ± standard deviation.

Results

Fabrication and characterization of nanopatterned PEG-GelMA-HA hydrogels

The chemical synthesis of PEG-GelMA-HA hydrogels is shown in Figure 1A. PEG is a synthetic hydrogel that demonstrates nontoxic and nonimmunogenic properties in addition to tunable mechanical strength.[41] However, PEG does not exhibit any biological activity, which prevents cell binding to the scaffold. Therefore, the incorporation of cell-binding adhesion sites is necessary. Gelatin methacrylate (GelMA) is a popular biomaterial due to its ability to form hydrogel structures through photopolymerization.[42] Gelatin is denatured collagen containing sites that facilitate cell binding and adhesion while possessing matrix metalloproteinase-sensitive degradation sequences that allow cells to remodel the ECM. As a light polymerizable material,

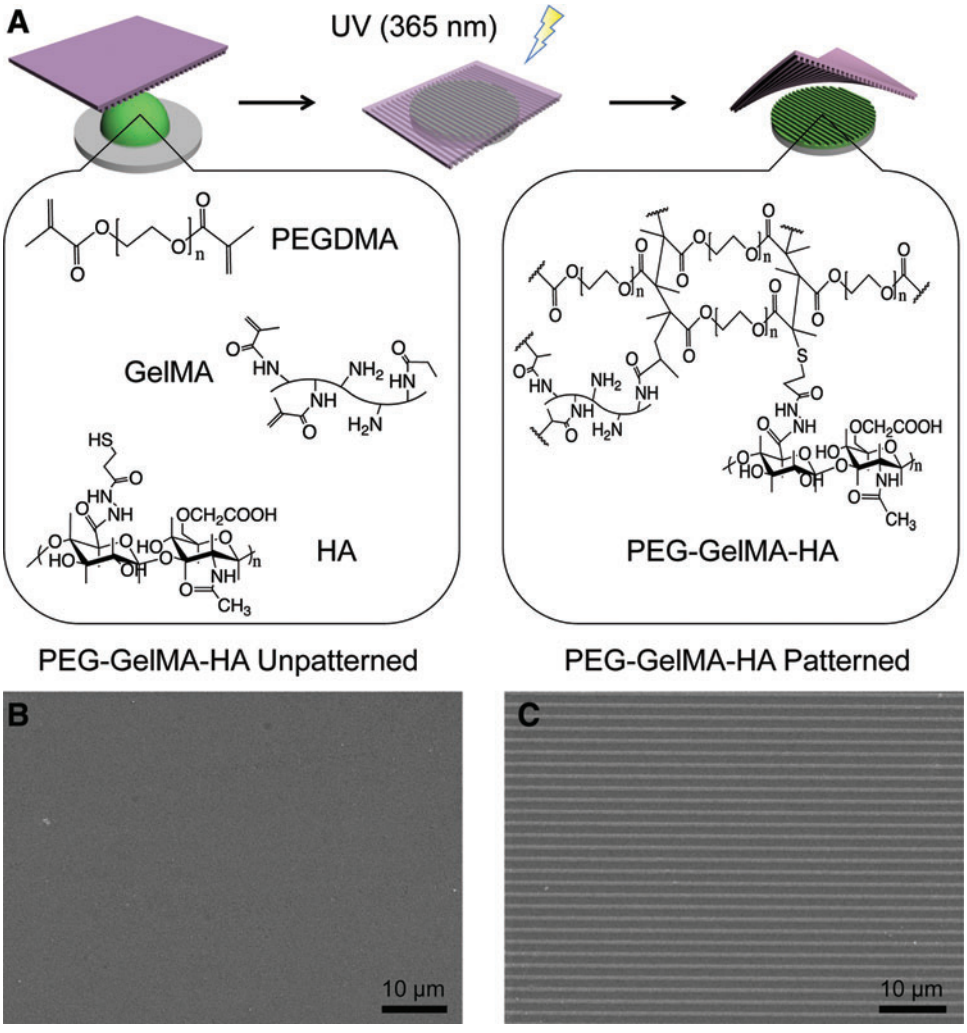

FIG. 1. Schematic of nanopatterned hydrogel synthesis. **(A)** PEG-GelMA-HA scaffolds were prepared from prepolymer mixture (green) consisting of poly(ethylene glycol) dimethacrylate (PEGDMA), methacrylated gelatin (GelMA), and thiolated hyaluronic acid (HA). The pattern was generated by using polyurethane acrylate (PUA) nanopattern (purple) and photopolymerization by low-wavelength ultraviolet light at 365 nm. **(B, C)** Scanning electron micrographs of PEG-GelMA-HA unpatterned and patterned hydrogels, respectively, with ridge × groove × height dimensions of 800 × 800 × 500 nm. Scale bars = 10 μm. Color images available online at www.liebertpub.com/tea

GelMA possesses the ability to be incorporated with other polymerizable materials such as PEGDMA to create tunable composite hydrogels that take advantage of both materials in terms of mechanical and biological profiles.[39]

A prepolymer solution containing PEGDMA, GelMA, and HA was cured by UV light to promote conjugation of GelMA and HA to the PEGDMA backbone through photopolymerization. To form nanopatterned scaffolds, a few drops of the prepolymer solution were dispensed on a glass substrate, and a PUA mold was then placed on the surface, forming a conformal contact with the surface. The polymer structure was cured by UV light, and the PUA molds were removed from the surface leaving behind a nanopatterned PEG-GelMA-HA scaffold. To confirm physical integrity and the presence of the nanotopography, SEM images were obtained from the PEG-GelMA-HA hydrogels prepared in unpatterned and nanopatterned conditions (Fig. 1B, C). The unpatterned PEG-GelMA-HA hydrogels contained no signs of altered topography, whereas the nanopatterned PEG-GelMA-HA hydrogels were composed of an array of linear grooves with ridge × width × height groove dimensions of $800 \times 800 \times 500$ nm as verified by analysis of the SEM images. The fabricated pattern was highly reproducible between experiments. The dimension choice of $800 \times 800 \times 500$ nm of the nanopattern demonstrated a high reproducibility in repeated fabrication. In addition, previous studies showed that anisotropic topographical scaffolds for superficial cartilage tissue engineering explored ranges within 500–1000 nm with success in inducing alignment of cells.[33,34]

To further verify the surface conjugation of HA, toluidine blue staining and XPS analysis were used. The toluidine blue staining revealed a homogenously intense blue color in the PEG-GelMA-HA scaffolds (Supplementary Fig. S2A) due to the presence of HA, whereas none appeared on the PEG-GelMA scaffolds (Supplementary Fig. S2B). The quantification of positive toluidine blue staining revealed that positive staining was highly significant for PEG-GelMA-HA compared with PEG-GelMA (***$p < 0.001$) (Supplementary Fig. S2C). XPS analysis demonstrated the presence of HA in HA-conjugated nanopatterned scaffolds, but not in nanopatterned scaffolds due to the presence of elevated nitrogen content (Table 1). This is to be expected as HA possesses nitrogen atoms. This provides evidence to support the conjugation of HA in the hydrogels.

Table 1. Atomic Mass Percentage of Carbon (C), Nitrogen (N), Oxygen (O), and Silicon (Si) Elements for Representative PEG-GelMA and PEG-GelMA-HA Samples

	Atomic conc. %			
Sample	*C*	*N*	*O*	*Si*
PEG-GelMA	67.6	4.0	27.2	1.2
PEG-GelMA-HA	65.9	5.1	27.3	1.7

Note that atomic mass percentage was determined by XPS analysis from a single spot of representative PEG-GelMA and PEG-GelMA-HA samples.

XPS, X-ray photoelectron spectroscopy; PEG, poly(ethylene glycol); GelMA, methacrylated gelatin, HA, hyaluronic acid.

Morphological analysis of DPSCs cultured on different scaffolds

To evaluate the biocompatibility of fabricated scaffolds, WST-1 assays of DPSCs after 24-h seeding on scaffolds were performed. The result showed no statistically significant difference in cell viability compared among cells seeded on scaffolds and TCPS (Supplementary Fig. S3), indicating no cytoxicity of our scaffolds. DPSCs were also able to attach on scaffolds and represented spindle-shaped cells, the morphology of MSCs (Fig. 2A, B). These results indicated that our fabricated scaffolds were not toxic to DPSCs.

The cell alignment and elongation were performed to indicate that cells responded to the nanotopographical cues provided by our fabricated scaffolds. The morphology of DPSCs cultured on unpatterned versus nanopatterned scaffolds is also an important aspect of mechanoregulation. After 24-h cell seeding, a confluent layer of DPSCs with random cellular orientation was observed on unpatterned PEG-GelMA-HA scaffolds, whereas a parallel cell alignment (indicated by a white arrow) was present on nanopatterned scaffolds (Fig. 2A, B). CD44, a cell surface receptor that binds HA and modulates cartilage differentiation, was stained in DPSCs cultured on unpatterned and nanopatterned PEG-GelMA-HA scaffolds, respectively (Fig. 2C, D).[43,44] DPSCs cultured on nanopatterned PEG-GelMA-HA scaffolds showed stronger CD44 staining at the cellular membrane following the orientation of the patterned scaffold compared with diffused CD44 staining by cells on unpatterned scaffolds. This increased membrane-localized CD44 staining following the orientation of the pattern on the scaffold suggests that CD44 on the cells is binding to HA on the patterned scaffolds and this binding may trigger signaling important for chondrogenesis. In addition, cellular alignment (indicated by a white arrow) was observed as expected for nanopatterned scaffolds compared with unpatterned scaffolds. DPSCs cultured on unpatterned scaffolds exhibited a cellular morphology with characteristics of random cell alignment. DPSCs cultured on nanopatterned scaffolds, however, exhibited a much higher frequency of alignment (Fig. 2E). There were no differences in the elongation of cells depending on the location on the patterned scaffolds. Moreover, the cellular elongation ratio determined by the length/width ratio demonstrated that DPSCs cultured on PEG-GelMA-HA patterned scaffolds had a significantly greater elongation than DPSCs cultured on unpatterned scaffolds (***$p < 0.001$) (Fig. 2F).

Effects of nanotopography and HA on spheroid formation

Spheroid formation was observed in both nanopatterned PEG-GelMA and nanopatterned PEG-GelMA-HA scaffolds. We also observed monolayer cells attached, elongated, and aligned along the pattern of scaffolds. DPSCs cultured on nanopatterned scaffolds were able to form spheroids after 24 h on top of elongated and aligned monolayer cells, while cells cultured on TCPS and unpatterned PEG-GelMA-HA scaffolds did not form spheroids (Fig. 3A–D). To differentiate live cells that form spheres from dead cells that form cell aggregates, we collected all floating spheres and replated on polystyrene surfaces. This would confirm if cells

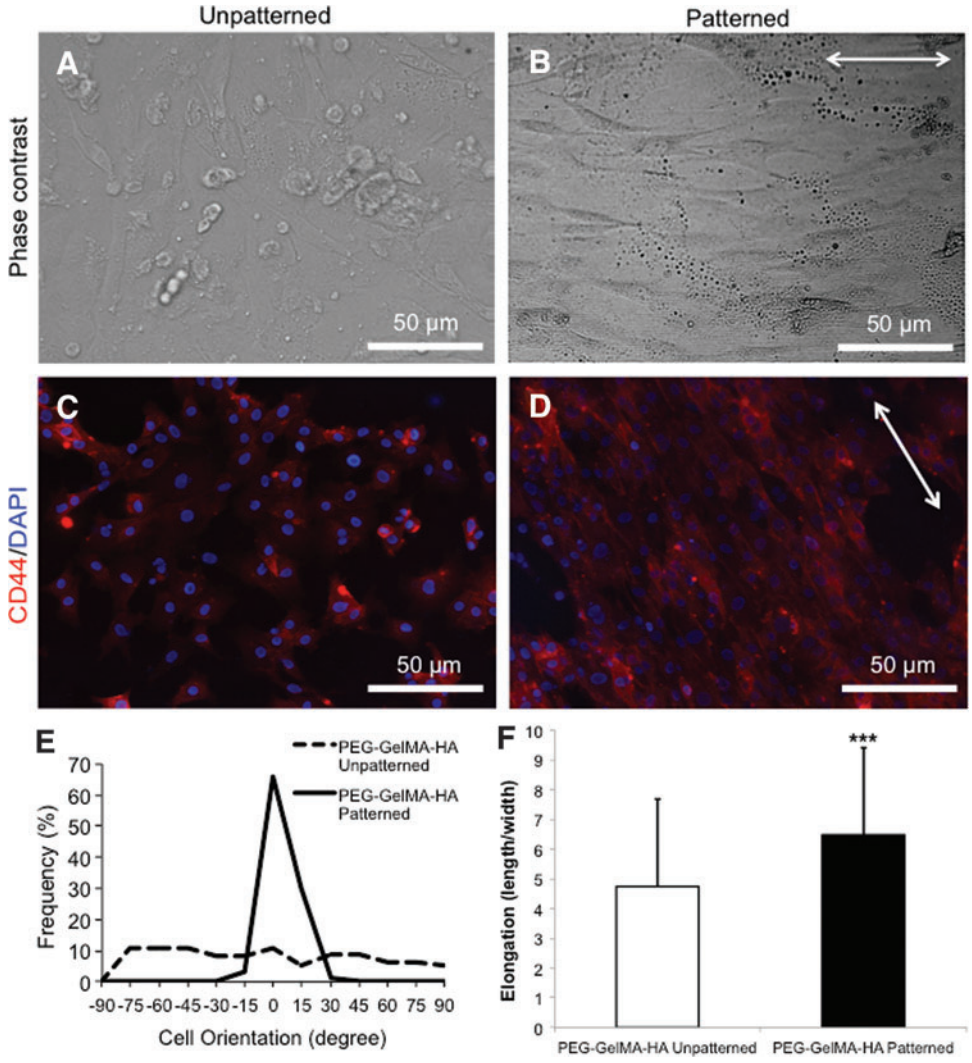

FIG. 2. The morphology of dental pulp stem cells (DPSCs) on different scaffolds. **(A, B)** Phase-contrast images of DPSCs seeded on PEG-GelMA-HA unpatterned and patterned, respectively. **(C, D)** CD44 staining of DPSCs seeded on PEG-GelMA-HA unpatterned and patterned, respectively, after 24 h. DPSCs aligned along nanopattern directions (indicated by the white arrows) on PEG-GelMA-HA patterned, but not on PEG-GelMA-HA unpatterned. Scale bars = 50 μm. **(E)** The cellular orientation (represented as percentage of frequency; $n = 100$) was determined for PEG-GelMA-HA unpatterned (dashed line) and patterned (solid line). **(F)** The cellular elongation (represented as a ratio between cell length/cell width; $n = 50$) was determined for PEG-GelMA-HA unpatterned and patterned scaffolds. Values are represented as mean ± standard deviation (SD) (***$p < 0.001$ with respect to PEG-GelMA-HA unpatterned) and analyzed by Student's *t*-test. Color images available online at www.liebertpub.com/tea

are alive or not. Live cells would attach on the surface, proliferate, and migrate. After replating all spheres, all of them were able to attach and proliferate until confluent. This result demonstrates that spheres formed in our scaffolds contained live cells.

Spheroids after 2 days attached to the TCPS surface and began to expand outward (Fig. 3E). Spheroids were continuously observed at day 6 after replating (Fig. 3F). The number of spheroids was also counted for each experimental group ($n = 3$) on day 2 and 6 postreplating (Table 2). Outward expansion continued until a confluent monolayer was formed (Fig. 3F) and resulted in a decrease in the number of spheroids at day 6, compared with that at day 2. Nanopatterned scaffolds with HA showed significantly greater numbers of spheroids compared with nanopatterned scaffolds without HA on both day 2 and 6 (***$p < 0.001$ and *$p < 0.05$, respectively). This indicated that nanopatterned topography itself enhanced the formation of spheres, but nanopattern and HA functioned synergistically to improve the capacity to form spheres. After *in vitro* differentiation, spheroids remained on the patterned scaffolds through 21 days and some spheroids, but not all, grew in size with time in culture.

Gene expression analysis of differentiated DPSCs

DPSCs seeded on TCPS and cultured in BMP-2 media exhibited significant upregulation of the chondrogenic-specific markers *Sox9*, *Alkaline phosphatase*, *Aggrecan*, and *Procollagen type II* after 21 days compared with cells cultured in growth media (*$p < 0.05$) (Supplementary Fig. S4), indicating that BMP-2 can induce *in vitro* chondrogenesis of DPSCs, as we have previously shown.[21]

To determine if fabricated scaffolds enhance the chondrogenic differentiation of DPSCs cultured in BMP-2 media, the expression of specific chondrogenic genes was analyzed at early (day 10) and late (day 21) time points. In nanopatterned scaffolds, the QRT-PCR results were analyzed in both monolayer and spheroids. At day 10, DPSCs cultured on different PEG-based scaffolds expressed higher levels of *Sox9*, *Alkaline phosphatase*, *Aggrecan*, and *Procollagen type II* and *X* compared with DPSCs cultured on TCPS (Fig. 4A–C and Supplementary Fig. S5). Among different kinds of scaffolds, DPSCs cultured on PEG-GelMA-HA patterned scaffolds expressed the highest level of chondrogenic genes. *Sox9*, *Aggrecan*, and *Procollagen type II* were significantly increased in the PEG-GelMA-HA patterned compared with

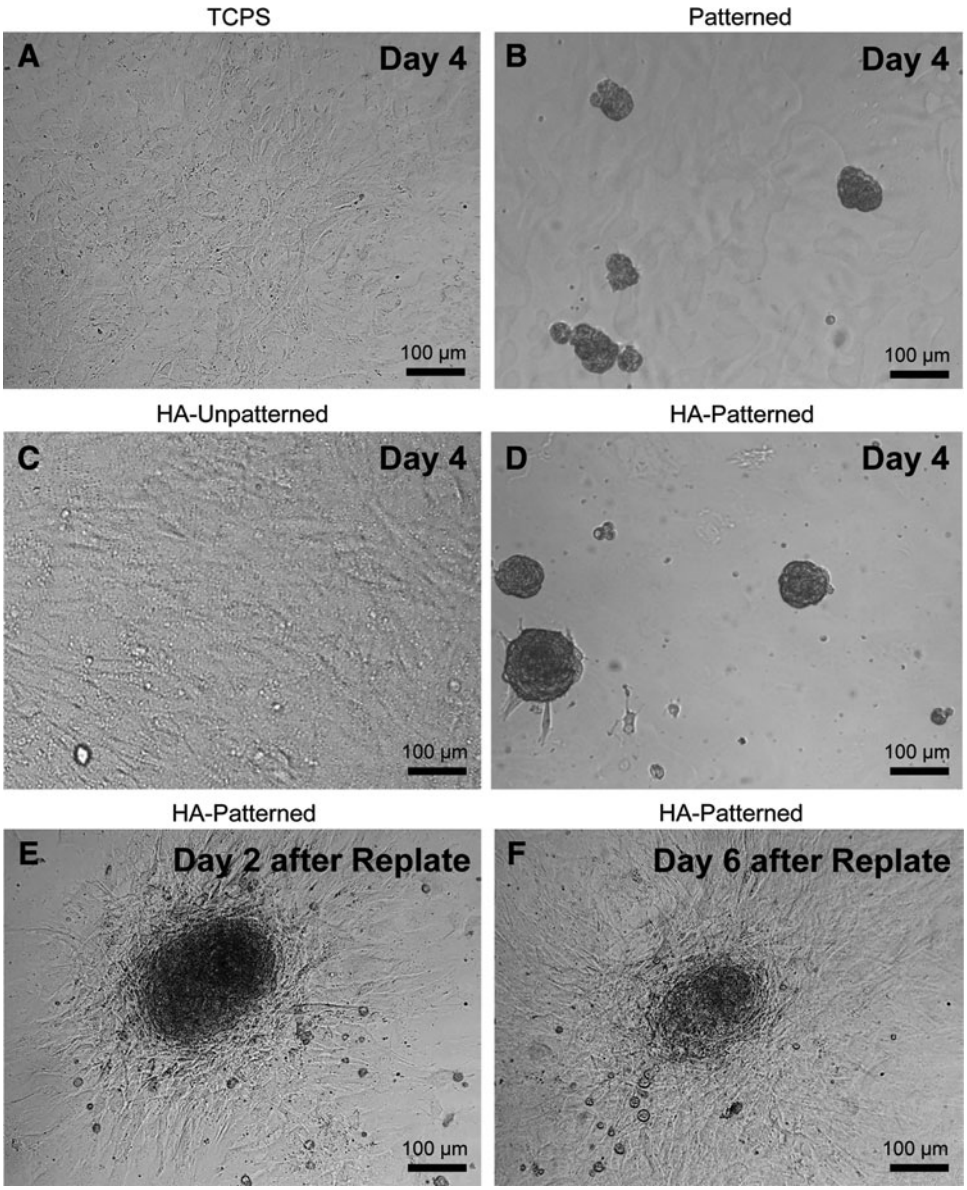

FIG. 3. DPSC-derived spheroid formation and viability on different scaffolds. **(A, C)** A confluent monolayer of DPSCs cultured in stem cell media after 4 days was observed in tissue culture polystyrene (TCPS) and PEG-GelMA-HA unpatterned scaffolds, respectively. **(B, D)** Spheroid formation observed on patterned PEG-GelMA and patterned PEG-GelMA-HA scaffolds after 4 days in stem cell media, respectively. Spheroids were collected from PEG-GelMA patterned and PEG-GelMA-HA patterned scaffolds and then replated on TCPS. **(E, F)** After 2- and 6-day replating, cell migration and proliferation were observed from a spheroid to the tissue culture plates as indicated by the decrease of spheroid size. Scale bars = 100 μm. Patterned, PEG-GelMA patterned; HA unpatterned, PEG-GelMA-HA unpatterned; HA patterned, PEG-GelMA-HA patterned.

TCPS and other scaffold groups (*$p < 0.01$). The expression of *Alkaline phosphatase* and *Procollagen type X* in DPSCs cultured on the PEG-GelMA-HA patterned scaffolds significantly increased when compared with that on TCPS, but did not differ from that on PEG-GelMA patterned and HA unpatterned scaffolds (*$p < 0.05$). The effect of PEG-based scaffolds on the chondrogenic differentiation of DPSCs was also assessed after 21 days. In contrast to that on day 10, *Sox9* was significantly downregulated in DPSCs cultured on PEG-based scaffolds, compared with TCPS (*$p < 0.01$). However, cells in HA-based scaffolds expressed significantly higher levels of *Sox9* than those on nanopatterned PEG-GelMA (*$p < 0.05$). At day 21, significant differences of chondrogenic genes were seen in HA-based scaffolds compared with TCPS, but there was no difference in *Alkaline phosphatase* and *Procollagen type X* in HA-based scaffolds. *Aggrecan* was significantly upregulated in DPSCs cultured on PEG-GelMA-HA scaffolds compared with TCPS and patterned PEG-GelMA scaffolds (Fig. 4B). Noticeably, *Procollagen type II* was expressed fourfold and sixfold higher in DPSCs cultured on PEG-GelMA-HA unpatterned and patterned scaffolds, respectively, compared with that on TCPS (*$p < 0.05$). Nevertheless, DPSCs cultured on PEG-GelMA-HA patterned scaffolds expressed significantly higher levels of *Procollagen type II* compared with that on PEG-GelMA-HA

Table 2. The Number of Spheroids from Different Nanopatterned Scaffolds After Replating on TCPS at Different Time Points

	Time of replate	
Sample	*2 days*	*6 days*
PEG-GelMA[a]	24[a]	18[a]
PEG-GelMA-HA	54[b]	32[a]

Value based on spheroids collected from three scaffolds each measuring 3.14 cm^2. Results were analyzed by Pearson's chi-squared test.

[a]$p < 0.05$ compared with PEG-GelMA at 2 days.

[b]$p < 0.001$ compared with PEG-GelMA at 6 days.

TCPS, tissue culture polystyrene.

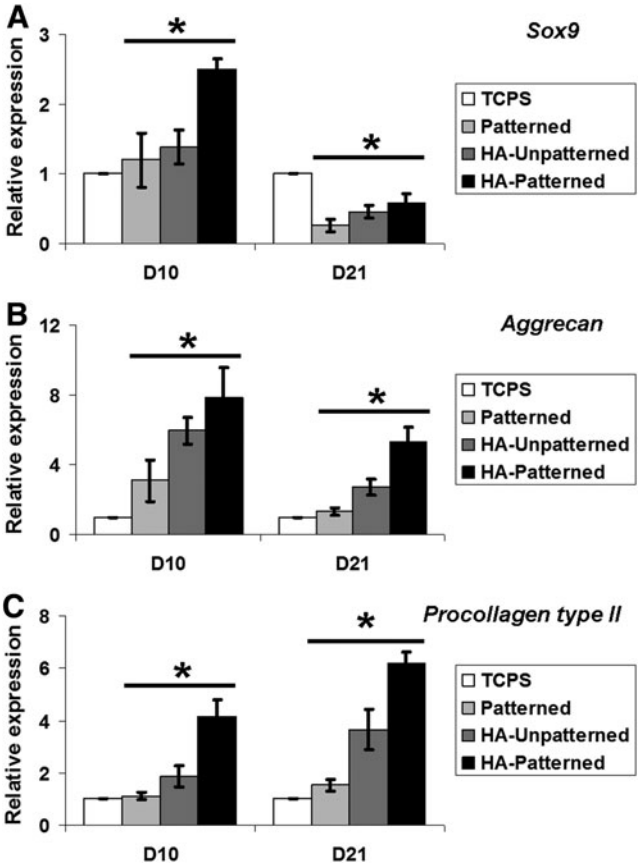

FIG. 4. Chondrogenic gene expression of DPSCs cultured on different scaffolds in bone morphogenetic protein (BMP)-2 media for 10 days (D10) and 21 days (D21). **(A–C)** At day 10 of differentiation, all chondrogenic genes were upregulated in DPSCs cultured on scaffolds compared with TCPS. *Sox9*, *Aggrecan*, and *Procollagen type II* were significantly increased in HA-scaffolds compared with patterned scaffolds. At day 21, *Sox9* was significantly downregulated in DPSCs cultured on poly(ethylene glycol) (PEG)-based scaffolds compared with cells on TCPS. *Aggrecan* and *Procollagen type II* were statistically significantly increased in DPSCs cultured on HA scaffolds compared with cells on TCPS and patterned scaffolds. Cells in HA patterned expressed significantly higher levels of chondrogenic genes than cells in HA unpatterned in 10 and 21 days. No significant difference in chondrogenic gene expression between cells on TCPS and patterned was seen at both time points. Values are represented as mean ± SD from three independent experiments ($n=3$), $*p<0.05$ with respect to indicated groups and analyzed by Student's *t*-test or one-way ANOVA.

unpatterned scaffolds ($*p<0.05$). There was no significant difference in chondrogenic gene expression between cells on unpatterned PEG-GelMA and TCPS.

DPSCs seeded on different scaffolds significantly increased the expression of *Nanog*, a pluripotent stem cell marker highly expressed by DPSCs,[21] compared with that on TCPS (threefold for patterned and HA, fourfold for HA patterned scaffolds). When cultured in BMP-2 media, DPSCs seeded on nanopatterned PEG-GelMA-HA scaffolds showed significantly lower *Nanog* expression compared

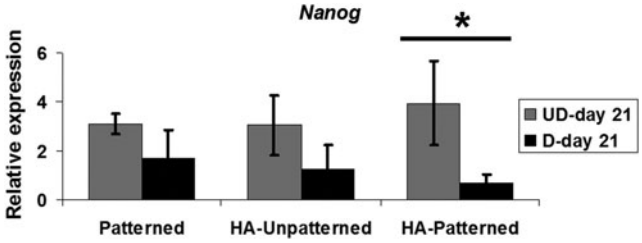

FIG. 5. *Nanog* expression of DPSCs cultured in growth media and BMP-2 media on different scaffolds for 21 days. DPSCs cultured in growth media on PEG-based scaffolds upregulated *Nanog* expression normalized to DPSCs cultured on TCPS. After chondrogenic differentiation, DPSCs seeded on PEG-based scaffolds showed decreased levels of *Nanog*. Only DPSCs plated on HA patterned scaffolds significantly decreased *Nanog* expression. Values are represented as mean ± SD from three independent experiments ($n=3$), $*p<0.05$ with respect to indicated groups and analyzed by Student's *t*-test.

with cells cultured in growth media on the same type of scaffolds, suggesting more efficient differentiation in this scaffold ($*p<0.01$) (Fig. 5).

Increased collagen type II protein expression of DPSCs on nanopatterned PEG-GelMA-HA scaffolds

Differentiated DPSCs cultured on TCPS stained positively for collagen type II (Fig. 6A), and DPSCs cultured on PEG-based hydrogel scaffolds revealed a stronger positive collagen type II staining compared with TCPS after 10 days (Fig. 6B–F). DPSCs cultured on nanopatterned PEG-GelMA and nanopatterned PEG-GelMA-HA scaffolds demonstrated positive staining not only in cell monolayers (Fig. 6B, E) but also in spheroids (Fig. 6C, F). The alignment of DPSCs cultured on nanopatterned scaffolds is indicated by white arrows. The IgG isotype showed a completely negative staining for collagen type II (Fig. 6G). ImageJ analysis was performed to determine the fluorescence positive staining per cell in each scaffold group (Fig. 6H). DPSCs cultured on scaffolds showed a greater positive staining of collagen type II staining compared with that on TCPS. However, only DPSCs cultured on unpatterned and nanopatterned PEG-GelMA-HA scaffolds showed significant differences in fluorescence staining ($***p<0.001$) compared with TCPS. DPSCs cultured on nanopatterned PEG-GelMA-HA scaffolds also significantly increased collagen type II membrane localization compared with that on patterned and HA ($***p<0.001$). In addition, we observed increased staining in spheroid areas (Fig. 6C, F) than in monolayer areas (Fig. 6B, D, and E), suggesting that the spheroids were chondrogenic.

Effect of HA on expression of Twist, Snail, *and* Slug *in DPSC-derived spheroids*

To gain insight into the potential mechanisms regulating chondrogenesis of DPSCs cultured on different scaffolds, mRNA expression of the EMT genes, *Twist*, *Snail*, and *Slug*, was determined by QRT-PCR in DPSC-derived spheroids on different scaffolds and replated cells cultured in stem cell

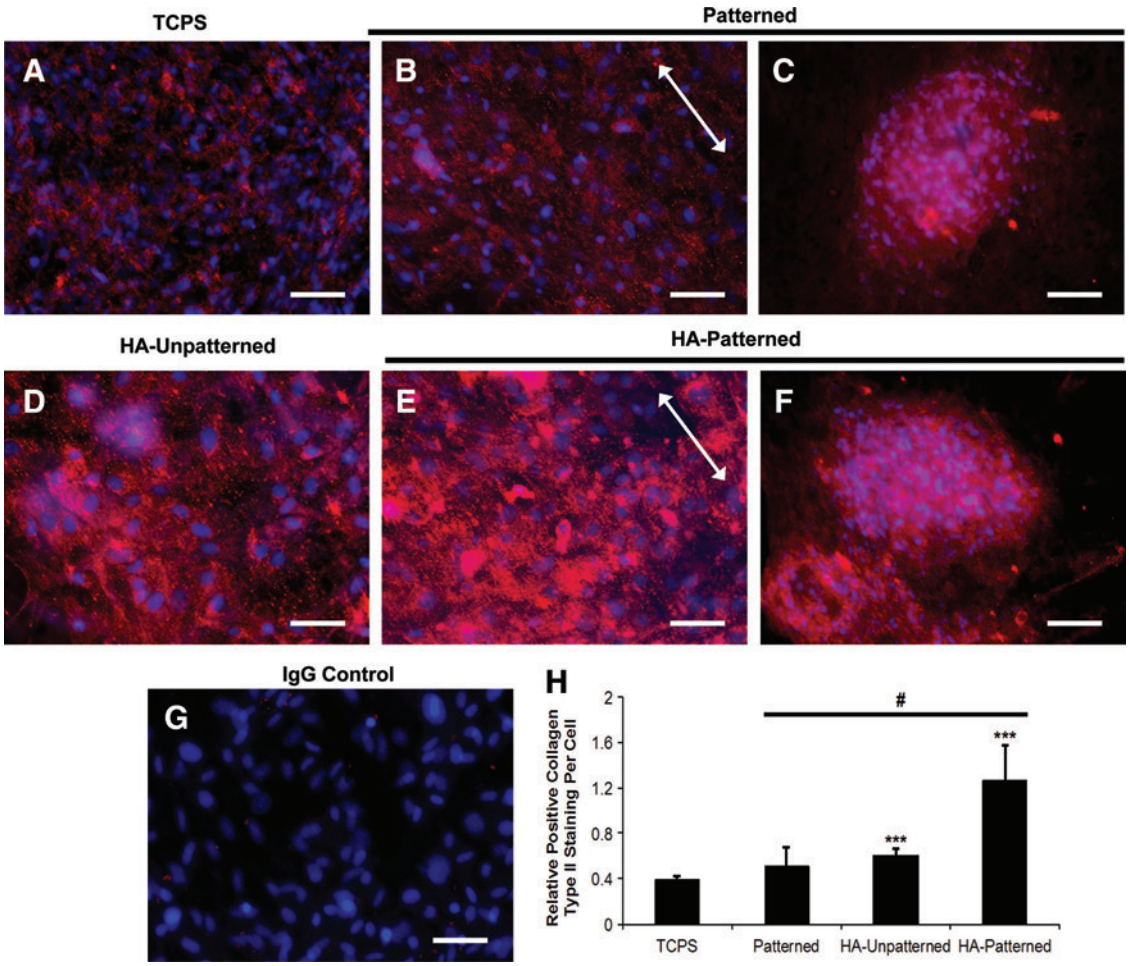

FIG. 6. Collagen type II staining of DPSCs on different scaffolds in BMP-2-media for 10 days. Positive collagen type II staining (in red) was observed in DPSCs cultured on TCPS **(A)**, patterned **(B, C)**, HA unpatterned **(D)**, and HA patterned **(E, F)**. **(G)** The IgG isotype was used as a negative control. Arrows indicate direction of pattern. Scale bars = 50 μm. **(H)** Positive collagen type II staining per cell (relative difference with respect to IgG isotype negative control) was quantified and compared between DPSCs cultured on different scaffolds. DPSCs cultured on HA patterned exhibited the significant strongest staining among all scaffolds. Values are represented as mean ± SD, $***p < 0.001$, with respect to indicated groups, and were analyzed by Student's *t*-test or one-way ANOVA. The number of samples for the image analysis was three samples per scaffold group ($n = 3$). From each scaffold, five images were used for the analysis. Color images available online at www.liebertpub.com/tea

media. We demonstrated that spheroid-derived cells and replated cells from patterned and HA patterned scaffolds significantly downregulated the expression of EMT genes compared with monolayer cells on TCPS. The level of EMT genes in replated cells was also significantly lower than that in spheroid-derived cells ($*p < 0.05$) (Fig. 7A, B). DPSC-derived spheroids collected from nanopatterned PEG-GelMA-HA scaffolds significantly downregulated the expression of all three EMT genes compared with those from nanopatterned PEG-GelMA scaffolds ($*p < 0.05$) (Fig. 7C). After replating, DPSCs from nanopatterned PEG-GelMA without and with HA scaffolds still expressed lower levels of EMT genes compared with cells on TCPS and spheroid-derived cells, indicating that the cells derived from the spheroids were already primed (induced) to the chondrogenic differentiation. Downregulation of EMT genes in DPSCs appears to be associated with enhanced chondrogenesis of DPSCs, which is influenced by HA. In addition to the EMT genes, undifferentiated cells on scaffolds expressed a significantly higher level of *Sox9*, a transcription factor for chondrogenesis, compared with undifferentiated cells on TCPS (Supplementary Fig. S6).

Discussion

The present study demonstrates the use of an easy and inexpensive platform that incorporates both topographical and chemical cues for chondrogenic differentiation of DPSCs. Numerous studies have demonstrated that the native ECM possesses nanoscale dimensions and chemical cues that govern cell regulation.[45,46] The incorporation of nano-topographical cues and HA as a potent chemical signal for chondrogenic differentiation has been investigated in previous literature.[47] Indeed, systems that incorporate topographical cues with HA demonstrate increased chondrogenic differentiation compared with individual parameters. However, these systems do not utilize well-ordered nanotopographies and have not assessed molecular chondrogenic

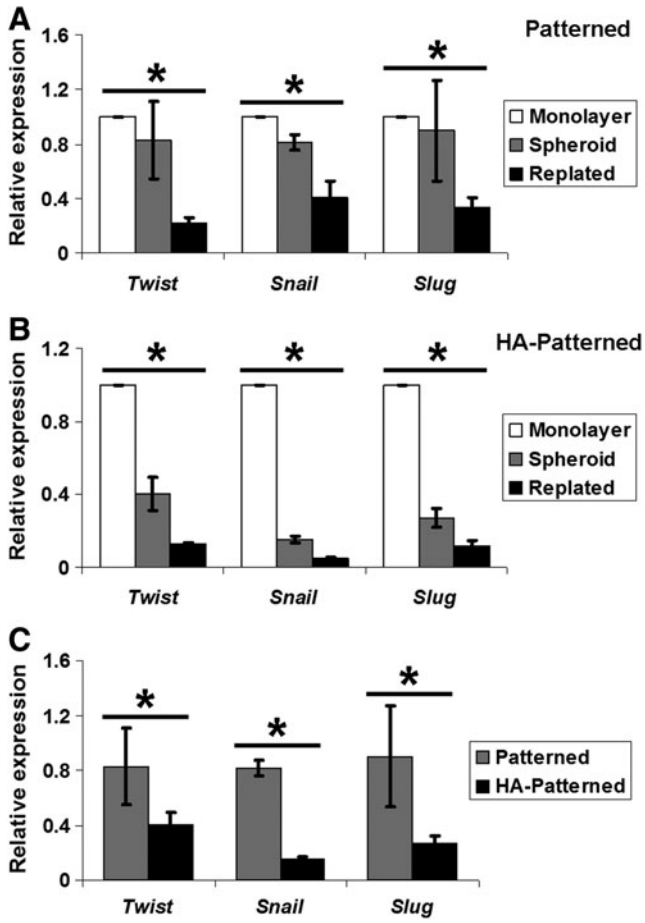

FIG. 7. The quantitative expression of epithelial–mesenchymal transition (EMT) genes (*Twist*, *Snail*, *Slug*) for DPSCs cultured on different scaffolds. The expression of *Twist*, *Snail*, and *Slug* was significantly decreased in DPSC-derived spheroids (Spheroid) in HA patterned. After replating on TCPS for 1 day, DPSC-derived monolayer cells (monolayer) from HA patterned still exhibited downregulated EMT genes, but only *Snail* was significantly decreased. Values are represented as mean ± SD, $*p < 0.05$ with respect to indicated groups.

differentiation potential in DPSCs, a promising postnatal stem cell source for chondrogenic differentiation that is easily obtained noninvasively and exhibits efficient *ex vivo* expansion and multidifferentiation capacity.[22,48]

High molecular weight HA cannot be used to easily generate nanopatterned scaffolds using CFL. PEG was thus used to successfully incorporate HA and form nanopatterns, whereas gelatin was further incorporated to provide necessary adhesion cues. We observed that DPSCs were not able to adhere and thus not able to survive (data not shown) on PEGDMA scaffolds without gelatin conjugated with or without HA. Consequently, we combined gelatin in PEGDMA scaffolds to have PEG-GelMA to promote cell adhesion. The results show that adding gelatin to the scaffolds enhanced cell attachment. Nevertheless, adding gelatin without HA did not enhance the *in vitro* chondrogenic differentiation of DPSCs. This is confirmed by no significantly statistical difference in gene and protein expression in DPSCs differentiated on TCPS compared with those on PEG-GelMA patterned scaffolds. After HA conjugation in patterned scaffolds, DPSCs were able to express higher levels of chondrogenic markers, suggesting that HA plays an important role in chondrogenic differentiation.

Previous studies show that both PEG-GelMA and PEG-RGD systems promoted cell adhesion.[39,49,50] However, in this study, we chose to use the PEG-GelMA system for its ability to be incorporated with other polymerizable materials, such as PEGDMA, to create tunable composite hydrogels that take advantage of both materials in terms of mechanical and biological profiles.

We observed that nanopatterned scaffolds induced morphological changes in the cultured DPSCs. The phase-contrast and CD44-stained imaging revealed that cells cultivated on nanopatterned scaffolds exhibited increased cellular elongation and preferential orientation parallel to the pattern. Our results are consistent with previous reports that utilized similar nanotopographical dimensions in their systems to promote cellular regulation and chondrogenic differentiation.[5,51,52] A previous study has shown that signaling triggered by binding of CD44 to HA is important for chondrogenesis as blocking with anti-CD44 antibodies inhibited chondrogenesis in adipose-derived stem cells.[53] Thus, the increased membrane-localized CD44 staining in cells on PEG-GelMA-HA scaffolds may indicate that CD44 is binding to HA and this binding triggers signaling for chondrogenic induction.

Furthermore, as chondrogenesis is favored in the 3D culture systems, such as the micromass technique or spheroid formation, we hypothesize that the role of nanotopography is to promote cell aggregation and extensive cell–cell contact formation to induce chondrogenic differentiation through formation of spheroid structures after initial contact with the scaffold. We previously demonstrated that nanopatterned polyurethane scaffolds further enhanced osteogenic differentiation of hMSCs with osteogenic induction media.[3,54] In this study, we first reported that nanopatterned PEG-GelMA-HA hydrogels promoted chondrogenic differentiation of DPSCs. Our scaffolds provide a nanotopographically defined 3D environment with grooves of 500 nm that creates depth in addition to the other two dimensions, width and length. This 3D nanotopographically defined environment promotes sphere formation, which mimics the natural rounded unattached environment of a chondrocyte. Plating chondrocytes on surfaces often results in dedifferentiation, and thus, plated MSCs often have unsuccessful chondrogenesis. To our surprise, we observed the formation of spheroids on the patterned scaffolds, which we report as a notable phenomenon on the nanopatterned scaffolds. DPSCs are a special type of MSCs derived from the cranial neural crest, and during embryonic development, neural crest cells form spheres as they delaminate from the neural tube and migrate cranially.[55] We observed increased numbers of sphere formation on the patterned scaffolds with and without HA, which indicates that the nanotopographically defined 3D environment provided by the patterned scaffold is important for sphere formation and may be mimicking the rounded unattached environment of chondrocytes. Further studies will be required to determine the mechanistic cause leading to spheroid formation.

We observed that DPSCs cultured on nanopatterned PEG-GelMA scaffolds, with and without HA, compared with DPSCs cultured on TCPS, were able to generate 3D spheroids. Interestingly, nanopatterned scaffolds containing HA produced a larger quantity of spheroids than did nanopatterned scaffolds without HA. This is consistent with previous studies reporting the effect of HA on enhancing spheroid formation.[23] Therefore, we hypothesize that nanotopography may help induce the initial spheroid formation, while HA, perhaps through CD44 binding, provides chemical cues that promote further formation and stabilization, which may promote a cellular state more optimal for chondrogenic differentiation.

Upregulation of chondrogenic markers typically indicates chondrogenesis. In the presence of BMP-2 media, DPSCs cultured on PEG-GelMA-HA scaffolds more efficiently differentiate into the chondrogenic lineage, as demonstrated by upregulation of chondrogenic genes and proteins compared with scaffolds without HA. Downregulation of *Sox9* has been demonstrated to be necessary for maturation of chondrocytes as it is an early marker for differentiation.[56] DPSCs cultured on TCPS at day 21 exhibited high levels of *Sox9*, yet expressed lower levels of other chondrogenic differentiation markers such as *Procollagen type II* than did DPSCs cultured on scaffolds containing HA. This indicates that DPSCs cultured on TCPS initiated chondrogenic differentiation, but did not further progress and mature into differentiated chondrocytes as did DPSCs cultured on scaffolds containing HA. We further found that the expression of *Alkaline phosphatase*, *Aggrecan*, and *Procollagen type II* and *X* was significantly higher in DPSCs cultured on nanopatterned PEG-GelMA-HA scaffolds than in DPSCs cultured on TCPS after 21 days. Among those chondrogenic markers, *Procollagen type II* and *X* are considered as two important markers for mature chondrocytes. Accordingly, in our study, differentiated DPSCs cultured on nanopatterned PEG-GelMA-HA scaffolds expressed a higher level of *Procollagen type II* and *type X*. As a result of increased *Procollagen type II* and *X* expression, we conclude that nanopatterned PEG-GelMA-HA scaffolds can efficiently facilitate chondrogenic differentiation of DPSCs induced with BMP-2. Immunofluorescent positive staining of collagen type II after 10 days of culture showed a significantly higher expression of collagen type II protein in DPSCs cultured on scaffolds with HA than in DPSCs cultured on TCPS. Nevertheless, only scaffolds with nanotopography and HA together produced the highest collagen type II protein of all the scaffolds thus further suggesting that both physical and chemical cues need to be present together to achieve the most efficient differentiation of DPSCs.

We have previously shown that murine DPSCs are derived from neural crest origin and express EMT genes *Twist, Snail*, and *Slug*.[21] Indeed, these genes are highly upregulated in neural crest cells during their migration.[57] Previous studies demonstrated that *Twist* inhibits *Sox9*, whereas *Snail* and *Slug* directly inhibit chondrogenesis by regulating the gene expression of *Procollagen type II (Col2a1)* and *Aggrecan*.[26,27] Our current results are consistent with these previous studies as we demonstrate that DPSCs cultured on nanopatterned PEG-GelMA-HA scaffolds formed spheroids and downregulated EMT gene expression, resulting in enhanced chondrogenic differentiation. Together, these findings suggest that the chemical properties of HA as a chondrogenic inducer may be mediated by inhibition of EMT genes *Twist*, *Snail,* and *Slug*. Future studies are needed to determine if HA chondrogenic induction is dependent on CD44 signaling and whether this signaling regulates EMT gene functions.

Our interpretation of the results is that during chondrogenesis, a process opposite to EMT is required, wherein *Twist* downregulation first leads to upregulation of *Sox9*, a master regulator of chondrogenesis, followed by downregulation of *Snail* and *Slug*, sequentially resulting in upregulation of *Procollagen type II* and *Aggrecan.* In our studies, EMT genes decreased in cells on HA patterned, compared with those on patterned scaffolds. This result indicates that HA is important for further chondrogenic differentiation perhaps mediated by downregulation of EMT genes.

Nanog, a pluripotent stem cell gene important for stemness maintenance, was significantly upregulated in DPSCs in all experimental groups compared with that on TCPS. This may indicate the persistence of a Nanog-expressing stem cell population on the scaffolds. Decreased Nanog levels are correlated with differentiation of stem cells toward specific lineages.[58] Accordingly, we observed significantly decreased Nanog expression in DPSCs cultured on nanopatterned PEG-GelMA-HA scaffolds after differentiation, thus indicating increased differentiation potential for DPSCs, which correlates with the downregulation of EMT genes and upregulation of chondrogenic markers.

The aim of this work was to demonstrate the utility of an easily generated tissue scaffold possessing topographical and chemical cues in tandem for chondrogenic tissue engineering. Whereas nanotopography alone did not significantly improve chondrogenic differentiation in DPSCs, an increased chondrogenic effect was observed upon combination of nanopatterned scaffolds with HA (Supplementary Fig. S7). Our study is the first to demonstrate that HA conjugated to nanopatterned scaffolds can enhance *in vitro* chondrogenic differentiation in DPSCs. Although we did not directly compare our method with the classic pellet culture to induce chondrogenesis, our model of synergistic effects of the nanopatterned scaffolds with HA, wherein the patterned scaffold induces generation of sphere formation and HA further induces chondrogenesis (Supplementary Fig. S7) may be mimicking similar conditions induced by the pellet culture system. Importantly, with our method, we can control biomimetic, anisotropic, topographical cues and chondrogenic cues (e.g., HA) to further enhance cartilage tissue engineering.

Conclusion

In this study, we utilized CFL to fabricate nanopatterned PEG-GelMA-HA scaffolds that provide physical and chemical cues to enhance chondrogenesis in DPSCs. The downregulation of *Nanog* and EMT genes, upregulation of chondrogenic genes, and positive staining of collagen type II indicate that nanopatterned PEG-GelMA-HA scaffolds can efficiently induce chondrogenic differentiation of DPSCs. Our findings suggest that the combination of nanotopography and HA signaling in scaffolds could be utilized to enhance cartilage tissue engineering.

Acknowledgments

D.H.K. thanks the Department of Bioengineering at the University of Washington for the new faculty startup fund. M.R. thanks the Departments of Laboratory Medicine and Pathology at the University of Washington for their support. This work was supported by International Collaborative R&D Program through KIAT grant funded by the MOTIE (N0000894).

Disclosure Statement

No competing financial interests exist.

References

1. Subramony, S.D., Dargis, B.R., Castillo, M., Azeloglu, E.U., Tracey, M.S., Su, A., and Lu, H.H. The guidance of stem cell differentiation by substrate alignment and mechanical stimulation. Biomaterials **34,** 1942, 2013.
2. Kim, D.H., Kshitiz, Smith, R.R., Kim, P., Ahn, E.H., Kim, H.N., Marbán, E., Suh, K.Y., and Levchenko, A. Nanopatterned cardiac cell patches promote stem cell niche formation and myocardial regeneration. Integr Biol (Camb) **4,** 1019, 2012.
3. You, M.H., Kwak, M.K., Kim, D.H., Kim, K., Levchenko, A., Kim, D.Y., and Suh, K.Y. Synergistically enhanced osteogenic differentiation of human mesenchymal stem cells by culture on nanostructured surfaces with induction media. Biomacromolecules **11,** 1856, 2010.
4. Jiang, T., Deng, M., James, R., Nair, L.S., and Laurencin, C.T. Micro- and nanofabrication of chitosan structures for regenerative engineering. Acta Biomater **10,** 1632, 2014.
5. Kim, D.H., Lipke, E.A., Kim, P., Cheong, R., Thompson, S., Delannoy, M., Suh, K.Y., Tung, L., and Levchenko, A. Nanoscale cues regulate the structure and function of macroscopic cardiac tissue constructs. Proc Natl Acad Sci U S A **107,** 565, 2010.
6. Lee, M.R., Kwon, K.W., Jung, H., Kim, H.N., Suh, K.Y., Kim, K., and Kim, K.S. Direct differentiation of human embryonic stem cells into selective neurons on nanoscale ridge/groove pattern arrays. Biomaterials **31,** 4360, 2010.
7. Park, H., Cannizzaro, C., Vunjak-Novakovic, G., Langer, R., Vacanti, C.A., and Farokhzad, O.C. Nanofabrication and microfabrication of functional materials for tissue engineering. Tissue Eng **13,** 1867, 2007.
8. Zhang, G.J., Tanii, T., Zako, T., Hosaka, T., Miyake, T., Kanari, Y., Funatsu, T., and Ohdomari, I. Nanoscale patterning of protein using electron beam lithography of organosilane self-assembled monolayers. Small **1,** 833, 2005.
9. Hirschfeld-Warneken, V.C., Arnold, M., Cavalcanti-Adam, A., López-García, M., Kessler, H., and Spatz, J.P. Cell adhesion and polarisation on molecularly defined spacing gradient surfaces of cyclic RGDfK peptide patches. Eur J Cell Biol **87,** 743, 2008.
10. Du, F., Wang, H., Zhao, W., Li, D., Kong, D., Yang, J., and Zhang, Y. Gradient nanofibrous chitosan/poly ε-caprolactone scaffolds as extracellular microenvironments for vascular tissue engineering. Biomaterials **33,** 762, 2012.
11. Kshitiz, Kim, D.H., Beebe, D.J., and Levchenko, A. Micro- and nanoengineering for stem cell biology: the promise with a caution. Trends Biotechnol **29,** 399, 2011.
12. Suh, K.-Y., Park, M.C., and Kim, P. Capillary force lithography: a versatile tool for structured biomaterials interface towards cell and tissue engineering. Adv Funct Mater **19,** 2699, 2009.
13. Gasimli, L., Linhardt, R.J., and Dordick, J.S. Proteoglycans in stem cells. Biotechnol Appl Biochem **59,** 65, 2012.
14. Laurent, T.C., Laurent, U.B., and Fraser, J.R. The structure and function of hyaluronan: an overview. Immunol Cell Biol **74,** A1, 1996.
15. Entwistle, J., Hall, C.L., and Turley, E.A. HA receptors: regulators of signalling to the cytoskeleton. J Cell Biochem **61,** 569, 1996.
16. Shu, X.Z., Liu, Y., Palumbo, F., and Prestwich, G.D. Disulfide-crosslinked hyaluronan-gelatin hydrogel films: a covalent mimic of the extracellular matrix for *in vitro* cell growth. Biomaterials **24,** 3825, 2003.
17. Toh, W.S., Lee, E.H., Guo, X.M., Chan, J.K., Yeow, C.H., Choo, A.B., and Cao, T. Cartilage repair using hyaluronan hydrogel-encapsulated human embryonic stem cell-derived chondrogenic cells. Biomaterials **31,** 6968, 2010.
18. Matsiko, A., Levingstone, T.J., O'Brien, F.J., and Gleeson, J.P. Addition of hyaluronic acid improves cellular infiltration and promotes early-stage chondrogenesis in a collagen-based scaffold for cartilage tissue engineering. J Mech Behav Biomed Mater **11,** 41, 2012.
19. Yoo, J.U., Barthel, T.S., Nishimura, K., Solchaga, L., Caplan, A.I., Goldberg, V.M., and Johnstone, B. The chondrogenic potential of human bone-marrow-derived mesenchymal progenitor cells. J Bone Joint Surg Am **80,** 1745, 1998.
20. Wang, W.G., Lou, S.Q., Ju, X.D., Xia, K., and Xia, J.H. *In vitro* chondrogenesis of human bone marrow-derived mesenchymal progenitor cells in monolayer culture: activation by transfection with TGF-beta2. Tissue Cell **35,** 69, 2003.
21. Janebodin, K., Horst, O.V., Ieronimakis, N., Balasundaram, G., Reesukumal, K., Pratumvinit, B., and Reyes, M. Isolation and characterization of neural crest-derived stem cells from dental pulp of neonatal mice. PLoS One **6,** e27526, 2011.
22. Gronthos, S., Mankani, M., Brahim, J., Robey, P.G., and Shi, S. Postnatal human dental pulp stem cells (DPSCs) *in vitro* and *in vivo*. Proc Natl Acad Sci U S A **97,** 13625, 2000.
23. Huang, G.S., Dai, L.G., Yen, B.L., and Hsu, S.H. Spheroid formation of mesenchymal stem cells on chitosan and chitosan-hyaluronan membranes. Biomaterials **32,** 6929, 2011.
24. Lee, S., An, S., Kang, T.H., Kim, K.H., Chang, N.H., Kang, S., Kwak, C.K., and Park, H.S. Comparison of mesenchymal-like stem/progenitor cells derived from supernumerary teeth with stem cells from human exfoliated deciduous teeth. Regen Med **6,** 689, 2011.
25. Miura, M., Gronthos, S., Zhao, M., Lu, B., Fisher, L.W., Robey, P.G., and Shi, S. SHED: stem cells from human exfoliated deciduous teeth. Proc Natl Acad Sci U S A **100,** 5807, 2003.
26. Seki, K., Fujimori, T., Savagner, P., Hata, A., Aikawa, T., Ogata, N., Nabeshima, Y., and Kaechoong, L. Mouse Snail family transcription repressors regulate chondrocyte, extracellular matrix, type II collagen, and aggrecan. J Biol Chem **278,** 41862, 2003.
27. Reinhold, M.I., Kapadia, R.M., Liao, Z., and Naski, M.C. The Wnt-inducible transcription factor Twist1 inhibits chondrogenesis. J Biol Chem **281,** 1381, 2006.
28. Brini, A.T., Niada, S., Lambertini, E., Torreggiani, E., Arrigoni, E., Lisignoli, G., and Piva, R. Chondrogenic potential of human mesenchymal stem cells and expression of Slug transcription factor. J Tissue Eng Regen Med 2013. [Epub ahead of print.] DOI: 10.1002/term.1772.
29. Tscheudschilsuren, G., Bosserhoff, A.K., Schlegel, J., Vollmer, D., Anton, A., Alt, V., Schnettler, R., Brandt, J., and Proetzel, G. Regulation of mesenchymal stem cell and

chondrocyte differentiation by MIA. Exp Cell Res **312,** 63, 2006.
30. Lee, M.H., Kang, J.H., and Lee, S.W. The significance of differential expression of genes and proteins in human primary cells caused by microgrooved biomaterial substrata. Biomaterials **33,** 3216, 2012.
31. Kim, D.H., Lee, H., Lee, Y.K., Nam, J.M., and Levchenko, A. Biomimetic nanopatterns as enabling tools for analysis and control of live cells. Adv Mater **22,** 4551, 2010.
32. Liu, S.Q., Tian, Q., Hedrick, J.L., Po Hui, J.H., Ee, P.L., and Yang, Y.Y. Biomimetic hydrogels for chondrogenic differentiation of human mesenchymal stem cells to neocartilage. Biomaterials **31,** 7298, 2010.
33. McCullen, S.D., Autefage, H., Callanan, A., Gentleman, E., and Stevens, M.M. Anisotropic fibrous scaffolds for articular cartilage regeneration. Tissue Eng Part A **18,** 2073, 2012.
34. Wise, J.K., Yarin, A.L., Megaridis, C.M., and Cho, M. Chondrogenic differentiation of human mesenchymal stem cells on oriented nanofibrous scaffolds: engineering the superficial zone of articular cartilage. Tissue Eng Part A **15,** 913, 2009.
35. Kim, D.H., Kim, P., Song, I., Cha, J.M., Lee, S.H., Kim, B., and Suh, K.Y. Guided three-dimensional growth of functional cardiomyocytes on polyethylene glycol nanostructures. Langmuir **22,** 5419, 2006.
36. Denker, A.E., Nicoll, S.B., and Tuan, R.S. Formation of cartilage-like spheroids by micromass cultures of murine C3H10T1/2 cells upon treatment with transforming growth factor-beta 1. Differentiation **59,** 25, 1995.
37. Hsu, S.H., Huang, G.S., Lin, S.Y., Feng, F., Ho, T.T., and Liao, Y.C. Enhanced chondrogenic differentiation potential of human gingival fibroblasts by spheroid formation on chitosan membranes. Tissue Eng Part A **18,** 67, 2012.
38. Otsuka, H., Nagamura, M., Kaneko, A., Kutsuzawa, K., Sakata, T., and Miyahara, Y. Chondrocyte spheroids on microfabricated PEG hydrogel surface and their noninvasive functional monitoring. Sci Technol Adv Mater **13,** 064217, 2012.
39. Nichol, J.W., Koshy, S.T., Bae, H., Hwang, C.M., Yamanlar, S., and Khademhosseini, A. Cell-laden microengineered gelatin methacrylate hydrogels. Biomaterials **31,** 5536, 2010.
40. Kiernan, J.A. Histological and Histochemical Methods: Theory and Practice. 3rd edn. Oxford; Boston: Butterworth Heinemann, 2000.
41. Lin, C.C., and Anseth, K.S. PEG hydrogels for the controlled release of biomolecules in regenerative medicine. Pharm Res **26,** 631, 2009.
42. Van Den Bulcke, A.I., Bogdanov, B., De Rooze, N., Schacht, E.H., Cornelissen, M., and Berghmans, H. Structural and rheological properties of methacrylamide modified gelatin hydrogels. Biomacromolecules **1,** 31, 2000.
43. Nicoll, S.B., Barak, O., Csóka, A.B., Bhatnagar, R.S., and Stern, R. Hyaluronidases and CD44 undergo differential modulation during chondrogenesis. Biochem Biophys Res Commun **292,** 819, 2002.
44. Ishida, O., Tanaka, Y., Morimoto, I., Takigawa, M., and Eto, S. Chondrocytes are regulated by cellular adhesion through CD44 and hyaluronic acid pathway. J Bone Miner Res **12,** 1657, 1997.
45. Stevens, M.M., and George, J.H. Exploring and engineering the cell surface interface. Science **310,** 1135, 2005.
46. Patel, S., Kurpinski, K., Quigley, R., Gao, H., Hsiao, B.S., Poo, M.M., and Li, S. Bioactive nanofibers: synergistic effects of nanotopography and chemical signaling on cell guidance. Nano Lett **7,** 2122, 2007.
47. Kim, I.L., Khetan, S., Baker, B.M., Chen, C.S., and Burdick, J.A. Fibrous hyaluronic acid hydrogels that direct MSC chondrogenesis through mechanical and adhesive cues. Biomaterials **34,** 5571, 2013.
48. Huang, A.H., Chen, Y.K., Lin, L.M., Shieh, T.Y., and Chan, A.W. Isolation and characterization of dental pulp stem cells from a supernumerary tooth. J Oral Pathol Med **37,** 571, 2008.
49. Wacker, B.K., Alford, S.K., Scott, E.A., Das Thakur, M., Longmore, G.D., and Elbert, D.L. Endothelial cell migration on RGD-peptide-containing PEG hydrogels in the presence of sphingosine 1-phosphate. Biophys J **94,** 273, 2008.
50. DeLong, S.A., Moon, J.J., and West, J.L. Covalently immobilized gradients of bFGF on hydrogel scaffolds for directed cell migration. Biomaterials **26,** 3227, 2005.
51. Yin, Z., Chen, X., Chen, J.L., Shen, W.L., Hieu Nguyen, T.M., Gao, L., and Ouyang, H.W. The regulation of tendon stem cell differentiation by the alignment of nanofibers. Biomaterials **31,** 2163, 2010.
52. Kim, D.H., Provenzano, P.P., Smith, C.L., and Levchenko, A. Matrix nanotopography as a regulator of cell function. J Cell Biol **197,** 351, 2012.
53. Wu, S.C., Chen, C.H., Chang, J.K., Fu, Y.C., Wang, C.K., Eswaramoorthy, R., Lin, Y.S., Wang, Y.H., Lin, S.Y., Wang, G.J., and Ho, M.L. Hyaluronan initiates chondrogenesis mainly via CD44 in human adipose-derived stem cells. J Appl Physiol (1985) **114,** 1610, 2013.
54. Kim, J., Kim, H.N., Lim, K.T., Kim, Y., Pandey, S., Garg, P., Choung, Y.H., Choung, P.H., Suh, K.Y., and Chung, J.H. Synergistic effects of nanotopography and co-culture with endothelial cells on osteogenesis of mesenchymal stem cells. Biomaterials **34,** 7257, 2013.
55. Dupin, E., and Coelho-Aguiar, J.M. Isolation and differentiation properties of neural crest stem cells. Cytometry A **83,** 38, 2013.
56. Pavlov, M.I., Sautier, J.M., Oboeuf, M., Asselin, A., and Berdal, A. Chondrogenic differentiation during midfacial development in the mouse: *in vivo* and *in vitro* studies. Biol Cell **95,** 75, 2003.
57. Duband, J.L., Monier, F., Delannet, M., and Newgreen, D. Epithelium-mesenchyme transition during neural crest development. Acta Anat (Basel) **154,** 63, 1995.
58. Takahashi, K., Tanabe, K., Ohnuki, M., Narita, M., Ichisaka, T., Tomoda, K., and Yamanaka, S. Induction of pluripotent stem cells from adult human fibroblasts by defined factors. Cell **131,** 861, 2007.

Address correspondence to:
Deok-Ho Kim, PhD
Department of Bioengineering
University of Washington
Box 355061
Seattle, WA 98195

E-mail: deokho@uw.edu

Morayma Reyes, MD, PhD
Department of Pathology
University of Washington
Box 358050
Seattle, WA 98195

E-mail: morayma@uw.edu

Received: October 1, 2013
Accepted: April 7, 2014
Online Publication Date: June 25, 2014